FROM McCLINTOCK? — MAY 13, 1993
SIMMONS

II. WAVELENGTH CALIBRATION AND GRATING DRIVE PERFORMANCE

II.1 PREFLIGHT CALIBRATION AND PERFORMANCE

II.1.1 WAVELENGTH SCALE

Wavelength Ranges

The wavelength scale for the UVS follows the standard equation for an Ebert-Fasie spectrometer:

$$m\lambda = 2d\sin(\theta)\cos(\phi) \qquad \text{(II.1)}$$

m = the order number of diffraction

λ = the wavelength in Angstroms

d = the grating spacing ($d^{-1} = 2400$ grooves / mm)

$\theta = (\beta + \alpha) / 2$

$\phi = (\beta - \alpha) / 2$

α and β are the angles of incidence and diffraction for the grating. ϕ, the half angle difference between β and α, is fixed by the monochromator case geometry for each channel.

Output wavelengths are selected by rotating the grating through the appropriate angle:

$$\theta = (\alpha_0 + n_0\Delta + n\Delta) + \phi = \alpha + \phi \qquad \text{(II.2)}$$

where α_0=0.095° is the grating offset angle, Δ=0.0225° is the grating step size, and n_0 and n are integers. In the standard UVS spectral modes the order number of diffraction is m=1 for the F and N channels and m=2 for the G channel. In these modes, the instrument microprocessor commands the grating through a range of steps n=0 to 527 (528 wavelength positions) with n_0=0 for the F channel and n_0=300 for the G and N channels. Table II.1 lists the value of ϕ for each channel as well as the starting and ending wavelengths for the standard scan modes.

TABLE II.1 UVS STANDARD SCAN RANGES

CHANNEL	ORDER	n_0	ϕ	θ	SCAN RANGE
G	2	300	9.119°	15.964° - 27.822°	1131.5 - 1920.1 Å
F	1	0	11.315°	11.410° - 23.268°	1616.5 - 3227.9 Å
N	1	300	13.507	20.352° - 32.210°	2818.1 - 4319.0 Å

The grating drive initializes its zero position at the end of each major science frame (60 2/3 seconds). At the beginning of the next frame it steps out n_0 steps (n_0 always positive) and begins a 528 step scan toward increasing wavelength. After it completes its positive scan the grating rotates n_1 steps and begins a 528 step scan toward decreasing wavelength. A two scan cycle is completed when the grating rotates through $-n_1$ steps to return to its initial position. A major science frame contains 7 pairs of these 528 position up/down scans. The values for n_0 and n_1 for the standard scans are: n_0=n_1=0 for F-F, n_0=300 and n_1=0 for G-G and N-N, and n_0=0 and n_1=300 for F-N and F-G.

The default values of n_0 and n_1 can be changed as part of a standard UVS instrument command. Allowable values for n_0 are $0 \leq n_0 \leq 428$. Values of n_1 can be positive or negative but must be consistent with the requirement that the grating not step outside the range $-.625° \leq \alpha \leq 21.51°$. (The grating drive has a mechanical fiducial which closes an electrical contact when the grating housing strikes a stop during fly-back. After electrical contact is made, the grating steps out approximately 40 steps to its nominal zero position which is also called the electrical fiducial. By setting $n_1 = -n_0 - x$ with $0 \leq x \leq 32$, the grating can be made to step to negative values of α on the down leg of a scan.) Any channel or pair of channels may be programmed to scan 528 step segments of the spectrum which are different from its standard range. The scan range can be the same or different for positive and negative legs of a single up/down pair. For example by specifying $n_0=100$ and $n_1=-100$ produces ranges of 2115.2 Å - 3677.3 Å and 1806.5 Å - 3391.0 Å respectively for the up/down legs of an N-N scan. The useful spectral coverage for these non standard scans is summarized in Table II.2.

TABLE II.2 UVS EXTENDED SCAN RANGES

CHANNEL	ORDER	n_0	ϕ	θ	SCAN RANGE
G	1	0	9.119°	8.494° - 16.396°	1215.3 - 2318.8 Å
F	1	0-428	11.315°	10.690° - 32.897°	1515.8 - 4438.2 Å
N	1	0-428	13.507	12.882° - 35.090°	1806.5 - 4658.0 Å

† Detector sensitivity for G channel limits the useful range to about 350 steps with $n_0=0$. Low detector sensitivity may also reduce the effective wavelength range for F to less than 4438.2 Å for most applications.

Accuracy and Stability

The wavelength scales for the F and N channels were established by fitting penray lamp spectra to the grating equation. These data were obtained by observing a scattering screen in order to illuminate the entire aperture and field of view of the instrument. In general it is possible to fit the derived wavelength scale to the observed line positions to within ± 0.3 grating steps (±0.9 Å) for 7 lines in each channel. The G channel wavelength scale was established by observing the position of the hydrogen Lyman alpha line produced by a collimator which filled the entire aperture but did not fill the field of view and by observing the position of N_2 lines from an electron lamp. Assuming the absolute position of the Lyman alpha line is correct, the wavelength scale for the G channel should also be accurate to ± 0.3 grating steps (±0.5 Å) because the grating rotates through the same angles for both the G and N standard scans. The pre launch wavelength scale predicts that Lyman alpha should appear in step 54.3.

Because the 2536 line is bright and easily observed it was used as the "standard" for tracking the grating drive absolute position reproducibility during pre flight testing. During the period from 1985 to 1988 the position of this line shifted from 297.6 steps to 296.2 steps. These changes can be

attributed to shifts in the mounting of the grating and Ebert mirror which occurred during various vibration tests which were conducted during that period. After final calibration and vibration qualification in April 1989 appeared in step 296.7. The pre launch wavelength scale predicts that this line should appear at step 296.6.

No specific tests were performed to determine the limit to the repeatability of grating position from scan to scan. However, experience has shown that centers for penray lamp lines typically repeat to ±0.1 step in data sets which are taken a few hours to a few days apart.

The grating control system (See Section II.1.2) has redundant solid state emitter-detector diode pairs which are used to detect a Moiré fringe pattern. One pair is designated as primary and the second is designated as backup. Values of θ listed in Table II.1 correspond to the primary pair. When the backup pair is used the value of θ at each grating step decreases by 0.043° corresponding to a shift of spectral features toward larger step numbers by approximately 1.9 steps.

$\alpha_0 = 0.095°$ $\alpha_0 = 0.052°$

prime pair backup pair

Diode pair selection is set by UVS uplink command and is echoed in word 10 of each 548 word UVS engineering/science record. Bit 4 high in word 10 ((word 10) and (16) = 16) corresponds to the backup pair. Bit 4 low corresponds to the primary pair.

Temperature Depencence

Values reported in Table II.1 were determined from measurements taken at temperatures of approximately 20°C. Data from various thermal vacuum qualification tests show that wavelength scale is sensitive to temperature change. During those tests the step position for a spectral feature was observed to decrease by about 0.03 steps per degree Centigrade decrease in temperature for temperatures in the range 0° to 20°C.

Grating drive temperatures can be estimated from two thermistor readings which appear in words 16 and 17 of each engineering/science record. For temperatures in the range -20°C < T < 20°C thermistor data numbers are related to temperature by:

$$T = DN/3 - 44.3 \qquad 73 \le DN \le 193$$

$$DN = 3T + 133 \qquad -20°C \le T \le 20°C$$

During laboratory testing at ambient temperature thermistor values were observed to be approximately 190 DN (T~19°C). During flight these values have been in the range 140 DN - 170 DN (T~2.3°C - 12.3°C).

The grating drive may make a discontinuous change in step position at very low temperatures. During thermal vacuum testing the positions of spectral lines were observed to shift by -10.5 steps when the instrument was operated at -30°C. This change corresponds to a shift of one complete

fringe cycle (64/6=10.66 steps See Section II.1.3) and is probably the result thermal contraction of the contact which determines the grating mechanical fiducial.

II.1.2 LINESHAPE AND SPECTRAL RESOLUTION

Theoretical Lineshape and Spectral Resolution

The output of the spectrometer for a monochromatic emission line defines the instrument lineshape (or profile). As the grating rotates it sweeps the image of the entrance slit across the exit slit and the lineshape is the convolution of that image with the exit slit.

$$L(\theta) = w'_{en} \otimes w_{ex} \qquad \text{(II.3)}$$

w'_{en} = the width of the entrance slit image (mm)

w_{ex} = the width of the exit slit (w_{ex} = 0.436 mm)

For the Galileo UVS image aberration can be neglected; therefore, the entrance slit image width is given by:

$$w'_{en} = w_{en}\frac{\cos(\alpha)}{\cos(\beta)} = w_{en}\frac{\cos(\theta-\phi)}{\cos(\theta+\phi)} \qquad \text{(II.4)}$$

Since $\alpha<\beta$ for the UVS geometry the convolution is a trapezoid with full width half maximum (FWHM) and a full width at the base(FWAB) given by:

$$L(FWHM) = w'_{en} \qquad \text{(II.5)}$$

$$\mathrm{L(FWAB)} = w'_{en} + w_{ex} \qquad \text{(II.5')}$$

The observed profile depends on both the lineshape and the distance the entrance slit image moves during a grating step. If the grating is rotated through angle Δ (one step) then the image of the entrance slit moves a distance Δx in the focal plane:

$$\Delta x = F\frac{\cos(\beta)+\cos(\alpha)}{\cos(\beta)}\Delta \qquad \text{(II.6)}$$

F = the focal length of the spectrometer (F = 125 mm)

and the ratios of line profile FWHM and FWAB to step size are given by:

$$\frac{w'_{en}}{\Delta x} = \frac{w_{en}}{F\Delta}\frac{\cos(\alpha)}{\cos(\alpha)+\cos(\beta)} = 8.88\frac{\cos(\alpha)}{\cos(\alpha)+\cos(\beta)} \qquad \text{(II.7)}$$

$$\frac{w'_{en}+w_{ex}}{\Delta x} = 8.88 \qquad \text{(II.7')}$$

Spectral resolution for the UVS is the product of the grating dispersion and the lineshape FWHM.

$$\Delta\lambda = \frac{d\cos(\beta)}{mF}w_{en}\frac{\cos(\alpha)}{\cos(\beta)} = \frac{d\cos(\alpha)w_{en}}{mF} \qquad \text{(II.8)}$$

$\Delta\lambda$ = instrument spectral FWHM (Å)

TABLE II.3 lists the range of values for the spectral resolution in Angstroms and the lineshape FWHM in grating steps and for the standard scan ranges.

TABLE II.3 LINESHAPE AND SPECTRAL RESOLUTION
STANDARD SCAN RANGES

CHANNEL	SCAN RANGE	SPECTRAL FWHM	LINESHAPE FWHM
G	1131.5 - 1920.1 Å	7.2 - 6.9 Å	4.6 - 4.8 STEPS
F	1616.5 - 3357.1 Å	14.5 - 14.2 Å	4.6 - 4.8 STEPS
N	2818.1 - 4319.0 Å	14.4 - 13.8 Å	4.8 - 5.1 STEPS

Gaussian Approximation

The image of the entrance slit is about 15% wider than the exit slit for the G and F channels and about 28% wider than the exit slit for the N channel. For this range of values the instrument lineshape is nearly triangular and can be approximated by a Gaussian profile. Figure II.1 illustrates the accuracy to which a Gaussian approximates the ideal instrument profile.

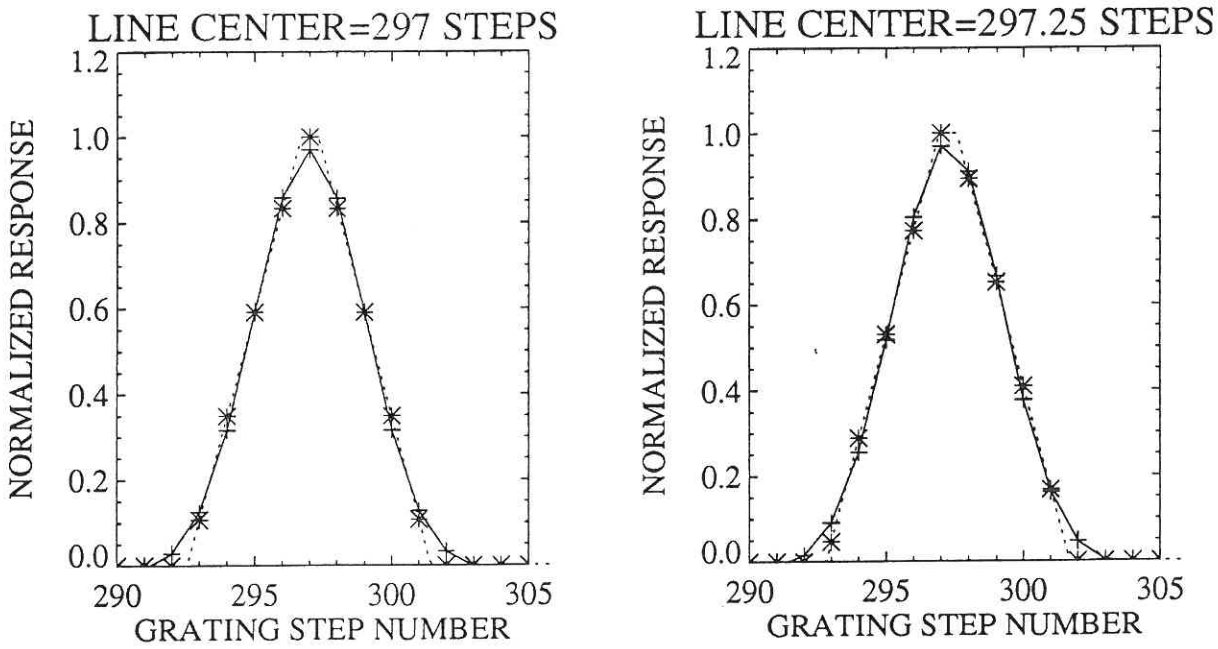

FIGURE II.1 Comparison of theoretical instrument profiles (solid lines) to Gaussian profiles (dashed lines). A Gaussian profile provides a very good approximation to the UVS lineshape which is nearly triangular over the entire wavelength range.

The dotted line represent the spectrometer response to a monochromatic line near the mid range of the F channel where $\alpha \sim 6.78°$ and $\beta \sim 29.41°$. For this configuration the theoretical profile is a

trapezoid with $w_{en'} = 1.15 w_{ex}$ and FWHM = 4.75 grating steps. The asterisks are the discrete samples taken at each grating step and the pluses connected by solid lines are nonlinear least squares fits of the sum of a Gaussian profile and a straight line to the samples. In general Gaussian fits predict line center for a theoretical profile to high precision. On the other hand, the line width estimates depend slightly on the details of the number of samples across the line and the position of line center. For example, when line center is located at step 297 (Figure II.1a) and at step 297.25 (Figure II.1b), the FWHM for the Gaussian fit is 4.79 steps and 4.76 steps respectively. Detailed parametric testing shows that FWHM estimated from Gaussian fits agree with the ideal profile FWHM to within ± 3% over the entire UVS wavelength range.

II.1.3 GRATING DRIVE DYNAMIC PERFORMANCE AND LINEARITY

Dynamic Performance

The data frame length for the Galileo UVS is 0.0076 sec. During a single frame the instrument logic integrates the detector output for times up to 0.006 sec and then issues a grating step command. The Galileo UVS grating drive responds to a step input with a settling time of about 0.02 sec. Because this time is about a factor of 3 larger than the frame length, the grating position always lags its nominal rest position.

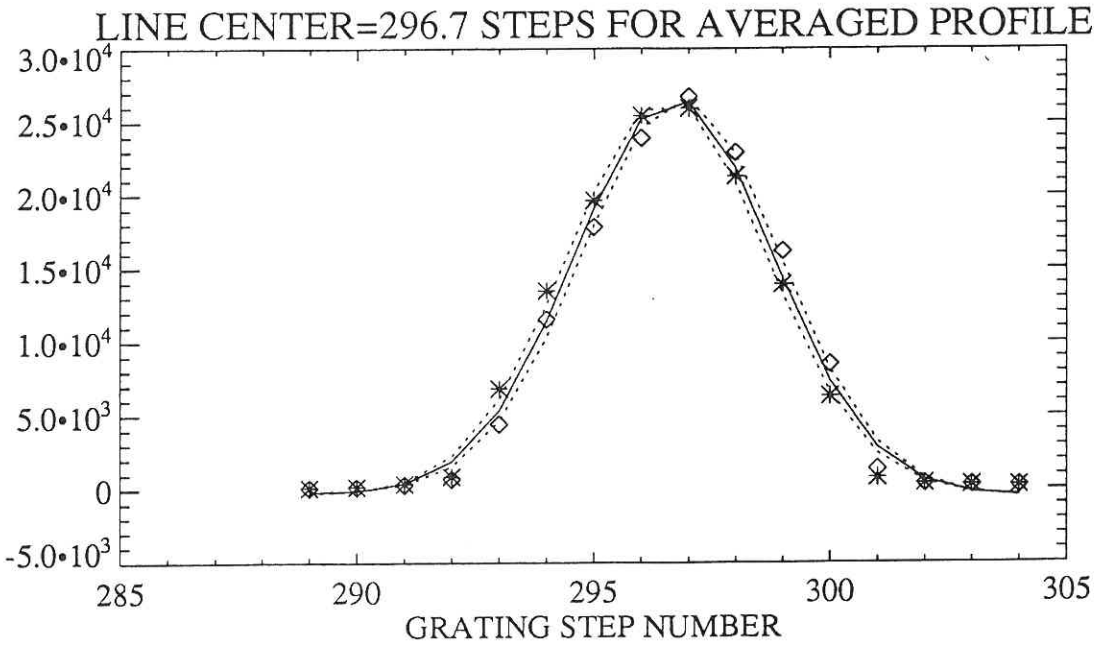

Figure II.2 Observed profile for the F channel. The line shape and FWHM agree with results derived in Section II.1.3 above. Two slightly offset profiles result from the dynamic response of the grating.

This lag causes spectra taken while the grating is scanning toward longer wavelengths to be shifted toward longer wavelengths relative to spectra taken while the grating is scanning toward shorter wavelengths. The magnitude of the shift is approximately 0.25 steps. Figure II.2 shows plots of laboratory wavelength calibration data taken with the F channel while the UVS viewed a $BaSO_4$ coated scattering screen which was illuminated with a mercury penray lamp. Asterisks mark the sum of 100 spectra which were accumulated while the grating was scanning toward longer wavelengths. Diamonds are the sum of 100 spectra accumulated while the grating was scanning toward shorter wavelengths. For clarity only 16 values near the 2536.52 Å line are shown in the figure. Dashed lines are the result of fitting a Gaussian plus linear profile to each data set.

Line centers and FWHM of the fitted profiles are 296.5 and 4.93 grating steps for the positive going sum and 296.8 and 4.90 steps for the negative going sum. The solid line is fit to the average of the two data sets for which the line center is 296.7 steps and the FWHM is 4.93 steps. The pre launch wavelength scale was established using the sum of positive and negative going spectra in principle a correction of ± 0.12 steps should be applied to data taken with the grating scanning only toward ± wavelengths.

Linearity

The grating drive uses a closed loop control system which counts optical fringes to measure the grating angular position. Fringe patterns are generated by overlaying two radial groove transmission gratings. One transmission grating is fixed, and the other rotates with the diffraction grating housing. The gratings have a ruling density of 1500 lines per 360°. As the housing rotates, two solid state emitter-detector diode pairs measure the phase of a Moiré fringe pattern generated by the two transmission gratings. A light-to-dark-to-light fringe cycle occurs for every 0.024° of rotation. The grating control electronics divide a single fringe cycle into 64 increments to produce single grating "phase steps" which are 0.00375° in size. Six phase steps are added to form a single spectral step Δ=0.0225°. For example, to reach the 2967 Å line in the F channel (centered at wavelength step 438.7) the grating moves through 439*6 phase steps which equals 41.156 fringe cycles.

This type of "incremental" grating drive may exhibit nonlinearities in step size as large as 10-15%. These nonlinearities arise from shifts in the phase of a single fringe which are caused by inexact placement of the solid state emitter-detector pairs, thermal drifts, and aging effects in the control electronics. They can usually be represented by one or two terms of a Fourier series which repeats from fringe cycle to fringe cycle so that the sum of 64 phase steps is always very close to 0.24°.

The magnitude of step size nonlinearity for the UVS grating drive was determined using the observed FWHM of the lines in the mercury penray lamp wavelength calibration spectra. Individual line widths measured in grating steps were then compared to values calculated using Equation II.7.

Consider the 2967 Å line. Equation II.7 predicts a FWHM of 4.78 steps for this line while the observed width is 4.19 steps. The ratio of observed to predicted width is 0.88. When the same line is observed using the N channel the grating must rotate through 32.815 fringe cycles and the ratio of observed to predicted width is 0.95. When the ratios of observed to calculated FWHM are plotted (Figure II.3) for both the F and N channels a simple pattern emerges which can be approximated by a sinusoidal function. The solid line in Figure II.3 is a nonlinear least squares fit of the equation

$$\frac{Observed\ FWHM}{Calculated\ FWHM} = A + B\sin(\frac{6N\pi}{32} + \phi) \qquad \text{II.9}$$

to the data. For this fit the amplitude of the step size non linearity varies over a range ±9.7% with a minimum occurring at substep 17.7.

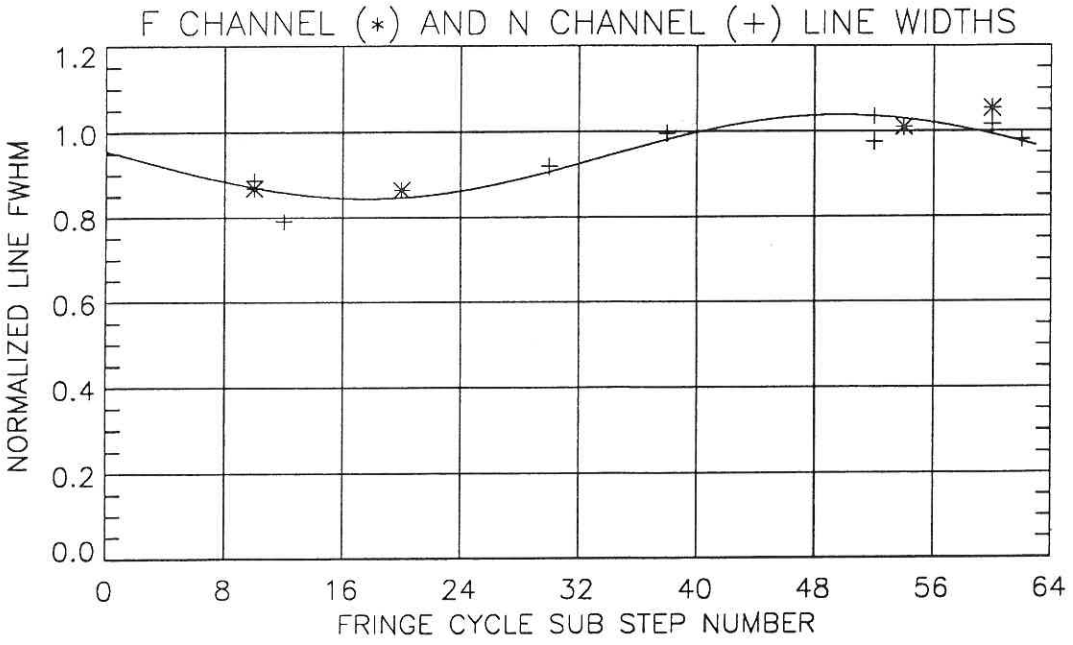

FIGURE II.3 Nonuniformity in the UVS grating drive step size. Nonuniform step size causes a variation in the observed FWHM monochromatic emission lines. This nonuniformity is a function of encoder fringe cycle position.

In principle nonlinearities in step size should also result in shifts of the position of spectral features. In practice this effect is difficult to observe with an emission line source because measured line center positions are only repeatable to about ± 0.1 steps while the maximum change in line position due to nonlinear step size is only 0.35 steps. Tests using mercury penray lamp wavelength calibration spectra demonstrated that equation II.1 fit the observed positions of lines equally well when the grating step size was fixed at Δ=0.0225° and when it was allowed to vary according to equation II.9.

II.2 FLIGHT PERFORMANCE

Short Term Stability and Temperature Sensitivity

Several data sets are available for characterizing the flight wavelength scale and performance of the grating drive. These include scans of interplanetary Lyman alpha, observations of the atmospheres of Venus and the Earth, and lunar observations made during the two Earth encounters.

Figure II.4 shows a typical example of the interplanetary Lyman alpha observations. These data were obtained with the instrument programmed to execute a 16 step mini-scan beginning at step 47 in the G channel. Each plot is the sum of data taken over a period of 72 minutes during the first third of the Earth 2 antisun map. The solid line in the left panel shows the data which were taken with the grating scanning toward longer wavelengths. The dashed line is the least squares fit of a Gaussian plus linear curve which has its line center at 54.02 steps and a FWHM of 4.52 steps. Results for data taken with the grating scanning toward shorter wavelengths are shown in the right panel. Based on Monte Carlo simulations, errors in the estimated values returned by the fitting routine for line center and FWHM for an observation in which the peak of the line has about 4000 counts are ±0.02 steps and ±0.05 steps respectively due to photon statistics.

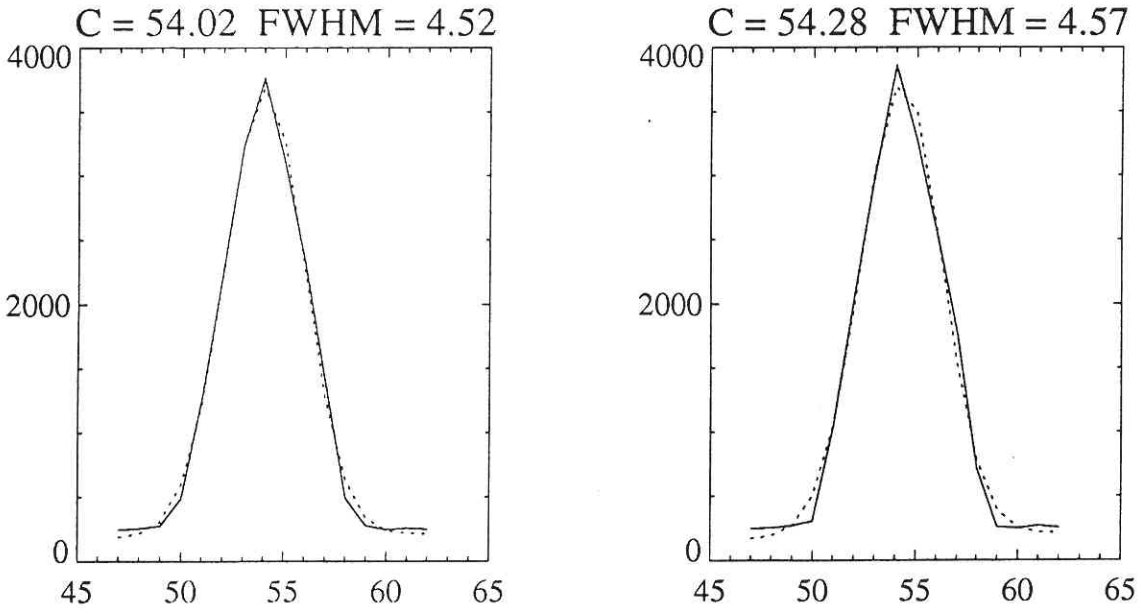

FIGURE II.4 Measurements of hydrogen Lyman alpha obtained during Earth 2 encounter. The solid lines are sums of scans obtained with the grating scanning toward increasing wavelength (left panel) and decreasing wavelength (right panel). Dashed lines are least squares fits of Gaussian profiles to the two data sets. Line center and FWHM for these Gaussians are shown above each plot.

Line center position for the sum of the two profiles is 54.15 steps. The measured FWHM is 4.55 steps compared to the value 4.52 predicted using equations II.7 and II.9.

Maps of interplanetary Lyman Alpha taken during the Earth 1 and Earth 2 encounters provide the best information about the short term stability of the grating drive. During the E2 antisun map the position of the average line center changed varied form 54.11 to 54.26 steps from the beginning to the end of the observation (a time period of approximately 24 hours). During that same period the instrument temperature monitors which are located inside the logic assembly and the detector head registered a monotonic increase. Figure II.5 shows a plot of line center versus logic temperature. Each data point is the result of fitting a Gaussian plus linear profile to the sum of an approximately 72 minute observation. Upper and lower curves represent data taken with the grating scanning toward decreasing (upper curve) and increasing (lower curve) wavelengths. Straight lines are linear least squares fits to the two data sets. Their average slope is 0.03 steps/DN.

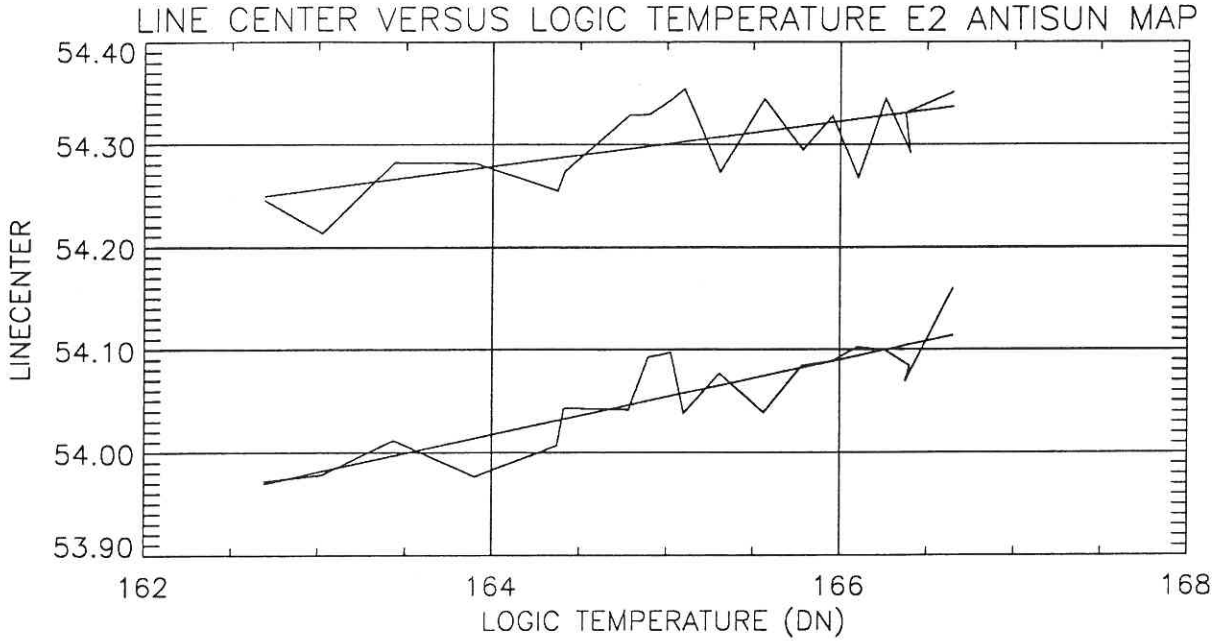

FIGURE II.5 The correlation between instrument logic temperature and line center position for the hydrogen Lyman alpha line observed during Earth 2 encounter. The upper (lower) plots are the sums of spectral scans for decreasing (increasing) wavelength.

Although there is a strong correlation of line position with temperature in this data set, there is evidence that small shifts in the wavelength scale caused by temperature changes in the instrument may be difficult to predict from the engineering data. The average slope of straight line fits in Figure II.5 is a factor of 3 larger than the slope derived during laboratory calibration. On the other hand, during a similar antisun map taken during the Earth 1 encounter the logic and detector temperature

monitors increased by 2 DN (compared to 4 DN for the E2 map) but the line center remained fixed over the entire observation.

As the instrument was heated and cooled slowly during calibration both temperature monitors were observed to have nearly identical readings suggesting that the instrument was always close to an isothermal state. In flight it appears that there may be temperature gradients within the instrument because the logic temperature monitor typically reads 10 DN (about 3° C) less than the detector temperature. Furthermore, as the instrument is rotated during any particular observation, it may be subjected to non uniform heat loads from solar illumination which could cause the monochromator case to deform. Another transient heat source may be arise from changes in power dissipated by other instruments on the scan platform.

Accurate correction of the absolute wavelength scale for temperature effects may require detailed knowledge of the solar illumination angle of the instrument and a record of any transient heat input form the spacecraft into the instrument.

Long Term Stability

Table II.4 summarizes a subset of flight observations of Lyman alpha which span the time from launch to Earth 2 encounter. Values for the least squares fit of a Gaussian plus linear fit to line center and FWHM are reported in columns 3, 4, and 5. Temperatures for the logic assembly and detector head in DN are shown in columns 6 and 7.

TABLE II.4 SUMMARY OF LYMAN ALPHA OBSERVATIONS

DATE	OBSERVATION	LINE CENTER		FWHM	LOGIC	DETECTOR
		$+\lambda$	$-\lambda$		TEMP	TEMP
4/27/88	PRE LAUNCH	54.2	54.4	4.5	190	190
12/10/89	FOUR DAY CHECKOUT	53.6	53.9	4.5	142	152
2/10/90	VENUS DAY GLOW		54.1	4.5	152	162
12/8/90	E1-EARTH DAY GLOW		54.3	4.5	162	172
12/8/90	E1-LUNAR RIDE 10		54.6	4.3	170	178
12/9/90	E1-LUNAR RIDE 15		54.3	4.5	174	181
12/13/90	E1-ANTISUN MAP	54.1	54.3	4.4	174	181
11/25/92	E2-ANTISUN MAP	54.0	54.3	4.6	165	173
12/9/92	E2-LUNAR DRIFT	54.1	54.3	4.6	169	176

Except for E1-Lunar Ride 10, all of the observations summarized in Table II.4 are consistent with a line center position which decreases with decreasing instrument temperature. Applying the

laboratory correction results in a line center of 54.3±0.1 steps for a combined profile with both increasing and decreasing wavelength scans.

The Lunar Ride 10 observation stands as a reminder that one should be cautious about interpretations of UVS data which require knowledge of the wavelength scale to better than ± 0.25 steps.

Solar Reflectance Spectrum Compared with UARS Observations

The Lunar Ride observations acquired during E1 provide an opportunity to characterize grating drive step size nonuniformity by comparing the reflected solar spectrum to direct observations of the sun made with the SOLSTICE experiment aboard the UARS. Results of this comparison are summarized in Figures II.6-II.7. The upper curve in the top half of Figure II.6 shows a typical 250 Å portion of the UVS Lunar Ride 15 observation of the moon (dashed line) compared to a solar spectrum obtained with Solstice (solid line). The solar spectrum was multiplied by a second order polynomial to normalize it to UVS detector counts. Differences in the two observations can be minimized by sliding the UVS data right or left to better match the solar data. The adjusted spectrum is compared to the Solstice spectrum in the lower pair of lines in the top half of the figure.

The bottom half of the figure shows how much the UVS data have been moved in order to make the best possible match to the solar spectrum for the wavelength range 2100 - 3250 Å. The ordinate is wavelength shift measured in grating step size (approximately 3Å per step). In most cases the data are shifted by less than 0.75 grating steps. Figure II.6 was plotted using a wavelength scale with the nonuniform grating step size described by Equation II.9. The magnitudes of the normalized deviations shown in the lower half of the figure are not significantly different from those which result from using a constant step size Δ=0.0225°.

Part of the deviation between the UVS and Solstice observations result from counting statistics in the lunar observations rather than errors in the UVS wavelength scale. Shifts caused by statistical fluctuations can be estimated by simulating a UVS observation using the solar data itself. In Figure II.7 the dashed line in the upper pair in the top half of the figure was generated from the solid line (i.e. the solar spectrum itself) by adding random Poisson distributed noise. Adjustments to the wavelength scale of required to minimize the differences between the solar observations and the simulated lunar observations are shown in the bottom half of the figure. They result from errors introduced by counting statistics rather than "errors" in the wavelength scale of the simulated data. In general their magnitudes are about 65% as large as those required to match the Lunar Ride 15 observations to the Solstice observations.

This exercise indicates that in general the wavelength shifts in the UVS data introduced by nonlinearities in the grating drive are on the order of ±0.25 steps or less. These shifts are only observable when the signal to noise ratio of the data approaches 100.

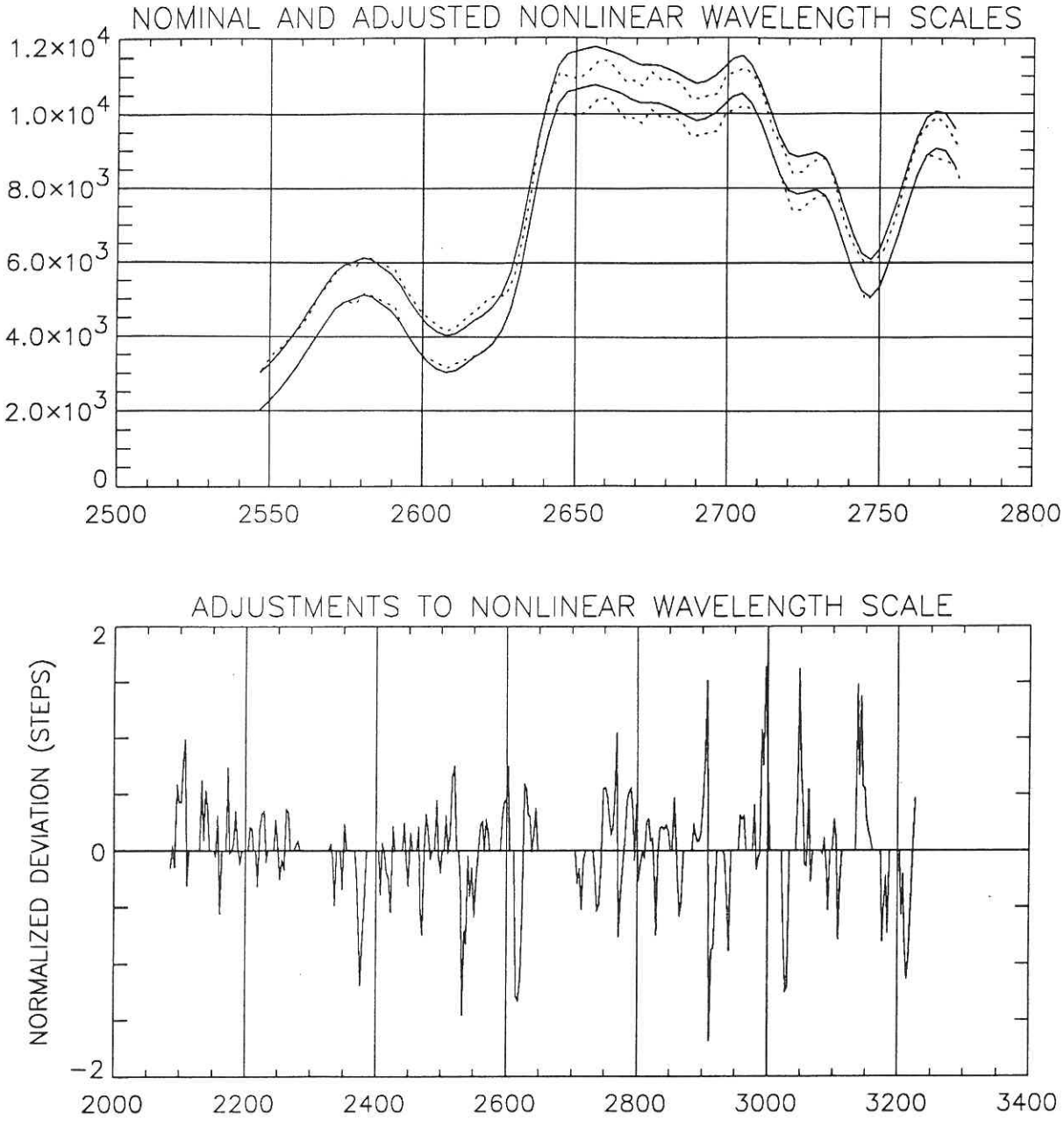

FIGURE II.6 The upper half compares a UVS lunar reflectance spectrum with a Solstice solar spectrum. Upper and lower curves show the comparison before and after the UVS wavelength scales were adjusted in order to minimize the differences between the two observations. The lower half is a plot of the adjustments to the UVS wavelength scale normalized to grating step size. Most adjustments are less than 0.75 steps in size.

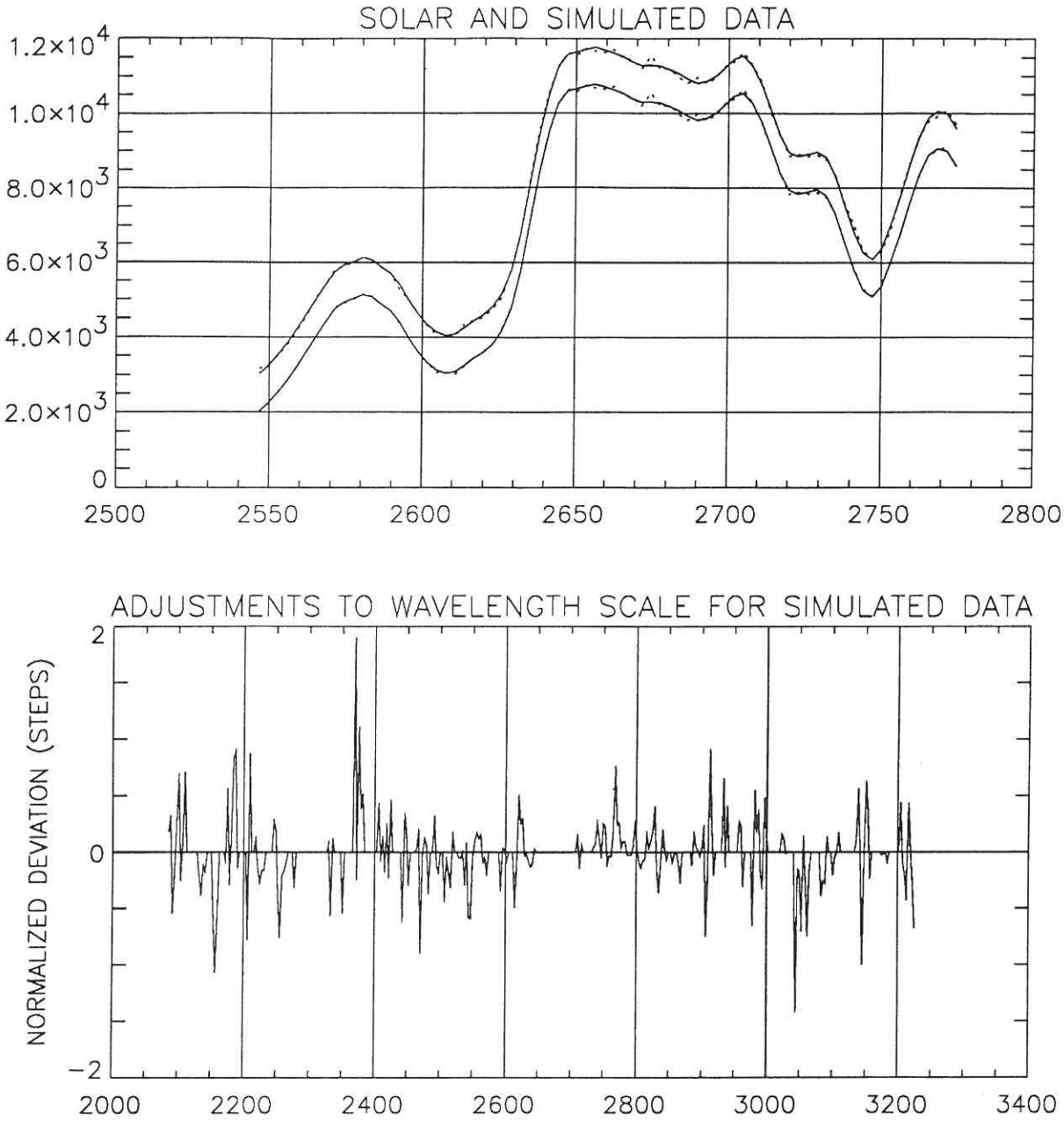

FIGURE II.7 The upper half compares a simulated UVS lunar reflectance spectrum with a Solstice solar spectrum. Adjustments in the wavelength scale of the simulated data required to make it fit the original observation are shown in the lower half. The magnitudes of these adjustments are on average 65% as large as those required when actual UVS data are used in the analysis.